

PROPAGATION OF THE BURST OF RADIATION IN EXPANDING AND RECOMBINING UNIVERSE: THOMSON SCATTERING

S.I.Grachev¹, V.K.Dubrovich^{2,3}

¹*Sobolev Astronomical Institute of Saint-Petersburg State University*

²*Saint-Petersburg department of Special Astrophysical Observatory of Russian Academy of Sciences*

Abstract. Within the framework of a flat cosmological model a propagation of an instantaneous burst of nonpolarized isotropic radiation is considered from the moment of its beginning at some initial redshift z_0 to the moment of its registration now (at $z = 0$). Thomson (Rayleigh) scattering by free electrons is considered as the only source of opacity. Spatial distributions of the mean (over directions) radiation intensity are calculated as well as angular distributions of radiation intensity and polarization at some different distances from the center of the burst. It is shown that for redshifts z_0 large enough ($z_0 \geq 1400$) the profile of the mean intensity normalized to the total number of photons emitted during the burst weakly depends on initial conditions (say the moment z_0 of the burst, the width and shape of initial radiation distribution in space). As regards angular distributions of intensity and polarization they turn to be rather narrow (3 – 10 arcmin) while polarization can reach 70%. On the average an expected polarization can be about 15%.

Key words: cosmology, early Universe, cosmological recombination, radiative transfer, Thomson scattering.

INTRODUCTION

Investigations of cosmic microwave background (CMB) both theoretical and experimental ones continue extensively all over the world. Achievements on this way are enormous. Information about fundamental parameters of the Universe is obtained. Contribution of completely new kind of matter inaccessible for investigation in ground based laboratories is discovered and measured. The main conclusions of the theory of origin of large scale structure of visible matter distribution in the Universe are confirmed. However the prospects of future investigations seem to be still more grandiose ones. In particular completely new discoveries are possible in the course of thorough studying of small scale CMB temperature fluctuations. Our paper is devoted to one of the mechanisms of such fluctuations.

In standard cosmological model fluctuations of matter density are possible on different scales – from very large to comparatively small ones. An interaction of these fluctuations with CMB during Universe expansion and cooling determines observed pattern of CMB temperature variations ($\Delta T/T$) at the moment of hydrogen recombination at a redshift $z \approx 1000$. Scales smaller than someones "damp" i.e. give very small values of $\Delta T/T$. This takes place for different reasons, namely through decrease of peculiar velocity of matter density fluctuation (cloud) due to radiation viscosity which leads to decrease of a Doppler shift of photons frequency; through

³E-mail: dvk47@mail.ru

decrease of cloud size relative to horizon and decrease of contribution of Sacks–Wolfe effect; through decrease of cloud optical thickness for Thomson scattering due to electron density decrease. However decrease of amplitude of the own matter density fluctuation takes place in this case for sonic waves only! At the same time for some class of fluctuations their contrast relative to surrounding matter increases. All these results are true for standard small density fluctuations. But we consider an evolution of $\Delta T/T$ for nonstandard models of origin of energy release on small scales. In particular this can be primary black holes, domains of different unstable forms of matter etc. at the epoch before hydrogen recombination. In such an aspect this problem was formulated in the paper by Dubrovich (2003). In the same paper an evolution of spatial distribution of "superequilibrium" radiation intensity was described qualitatively. Conclusion was obtained that an angular size of $\Delta T/T$ fluctuation observed now did not depend on a redshift of radiation source.

The aim of the present paper is a correct calculation of this process within the framework of standard theory of radiative transfer. As a model we use a source of sufficiently small size radiating during some small interval of time (instantaneously in particular). We assume that this radiation does not have any influence on the matter parameters (e.g. electron temperature and number density) during the whole process of scattering. Within the framework of the present paper we do not discuss an absolute quantity of scattered radiation intensity as well as its spectrum. Separate paper will be devoted to this question. We stress once more that we consider here completely different type of temperature inhomogeneity as compared with the standard scenario. Our source of inhomogeneity is not a small fluctuation of matter density described in the course of its evolution by equations of hydrodynamics and thermodynamics. Therefore conclusions of the standard theory of small scale fluctuations damping (Silk damping) are not applicable to it.

BASIC EQUATIONS

We consider nonstationary radiation transfer in homogeneous expanding Universe starting from spherically-symmetrical initial distribution of radiation intensity. For a flat model of the Universe the corresponding equation of radiation transfer for photon occupation number \vec{n} has the form (Nagirner, Kirusheva, 2005):

$$\frac{\partial \vec{n}}{\partial \eta} + \mu \frac{\partial \vec{n}}{\partial \rho} + \frac{1 - \mu^2}{\rho} \frac{\partial \vec{n}}{\partial \mu} - \frac{a \nu}{c} H \frac{\partial \vec{n}}{\partial \nu} = -a k (\vec{n} - \vec{s}), \quad (1)$$

where η is a conformal time ($d\eta = cdt/a(\eta)$, c is the speed of light, t is a time, $a = a(\eta)$ is a scale factor), ρ is a spatial coordinate, $H = H(\eta)$ is a Hubble factor, $\vec{n} = (c^2/2h\nu^3)(I, Q)^T$, $I = I(\rho, \mu, \eta, \nu)$ and $Q = Q(\rho, \mu, \eta, \nu)$ are Stokes parameters for radiation at a frequency ν propagating at an angle $\vartheta = \arccos \mu$ to radial direction, dimensionless vector source function is $\vec{s} = (s_I, s_Q)^T = (c^2/2h\nu^3)(S_I, S_Q)^T = (c^2/2h\nu^3)\vec{\varepsilon}/k$ and $\vec{\varepsilon} = \vec{\varepsilon}(\rho, \mu, \eta, \nu)$ and $k = k(\rho, \mu, \eta, \nu)$ are emission and absorption coefficients accordingly. It should be noted that $k = k(\eta)$ for Thomson scattering in a homogeneous medium. Here and further ^T means transpose.

Below we assume scale factor a to be equal 1 at the present epoch ($z = 0$) so that $a(z) = 1/(1+z)$ where z is a redshift. Therefore spatial coordinate ρ in eq. (1) is a distance from a center of symmetry measured in the present epoch (at $z = 0$). At an arbitrary z the corresponding distance is $r = \rho a(z) = \rho/(1+z)$. Further since Thomson scattering is neutral one

than radiation frequency ν changes due to cosmological redshift only: $\nu = \nu_0/a(z) = \nu_0(1+z)$, where ν_0 is a frequency at the present epoch. Therefore we may use ν_0 instead of ν as a frequency variable and we redefine the source function (Nagirner, Kirusheva, 2010) as follows:

$$\vec{n}(\rho, \mu, \eta, \nu) = \vec{n}_*(\rho, \mu, \eta, \nu_0) \equiv \vec{n}(\rho, \mu, \eta). \quad (2)$$

Then frequency variable disappears and eq. (1) takes the form

$$\frac{\partial \vec{n}}{\partial \eta} + \mu \frac{\partial \vec{n}}{\partial \rho} + \frac{1 - \mu^2}{\rho} \frac{\partial \vec{n}}{\partial \mu} = -k(\eta)a(\eta) [\vec{n}(\rho, \mu, \eta) - \vec{s}(\rho, \mu, \eta)]. \quad (3)$$

In the case of monochromatic scattering and in the presence of axial symmetry of radiation field the vector source function in the righthand side of this equation is written in the form

$$\vec{s}(\rho, \mu, \eta) = (1/2) \int_{-1}^{+1} d\mu' \hat{R}(\mu, \mu') \vec{n}(\rho, \mu', \eta), \quad (4)$$

where phase matrix $\hat{R}(\mu, \mu')$ describes radiation redistribution over directions and polarizations in a single scattering. For Thomson (Rayleigh) scattering phase matrix can be factorized as follows (see e.g. Ivanov, 1995):

$$\hat{R}(\mu, \mu') = \hat{A}(\mu) \hat{A}^T(\mu'), \quad (5)$$

where

$$\hat{A}(\mu) = \begin{pmatrix} 1 & \frac{1}{2\sqrt{2}}(1 - 3\mu^2) \\ 0 & \frac{3}{2\sqrt{2}}(1 - \mu^2) \end{pmatrix}. \quad (6)$$

In this case eq. (4) takes the form

$$\vec{s}(\rho, \mu, \eta) = \hat{A}(\mu) \vec{s}_*(\rho, \eta), \quad (7)$$

where

$$\vec{s}_*(\rho, \eta) = (1/2) \int_{-1}^{+1} \hat{A}^T(\mu') \vec{n}(\rho, \mu', \eta) d\mu'. \quad (8)$$

Eq. (3) looks like an ordinary nonstationary equation of monochromatic radiation transfer in a medium with the volume absorption coefficient

$$\alpha(\eta) = k(\eta)a(\eta), \quad (9)$$

which depends on time only. Therefore η/c can be considered as an ordinary time and ρ as an ordinary radial distance in the problems of nonstationary radiative transfer in spherically-symmetrical extended media. Thus we can use the method suggested earlier by Ivanov (1995) for solving problems of stationary transfer in plane-parallel media with generalized Rayleigh scattering. The method consists in reducing the problem to getting and solving an integral equation for so called reduced source function defined by eq. (8) which does not depend on angle variable. After that radiation field with its angular structure is defined from the formal (i.e. with the known source function) solution of initial eq. (3).

To obtain above mentioned formal solution we consider propagation of radiation along a ray intersecting radial direction at an angle $\vartheta = \arccos \mu$ at a distance ρ from the center of symmetry. Let us introduce coordinate l measured along a ray from the point nearest to the

center of symmetry in direction of radiation propagation. The lefthand side of eq. (3) is nothing else than derivative along the ray direction so that this equation is rewritten as

$$d\vec{n}/dl = -\alpha(l)[\vec{n}(l) - \vec{s}(l)]. \quad (10)$$

Integrating this equation we obtain

$$\vec{n}(l) = \vec{n}_0(l_0)e^{-\int_{l_0}^l \alpha(l')dl'} + \int_{l_0}^l \alpha(l')\vec{s}(l')e^{-\int_{l'}^l \alpha(l'')dl''} dl'. \quad (11)$$

Here l_0 is a coordinate of a point farthest from the observation point l but yet capable of making a contribution to radiation in this point at a given time η . Each point l' on a ray is defined by radial distance ρ' and by an angle $\arccos \mu'$ at which the ray intersects radial direction. It follows from geometry of the problem that

$$l = \rho\mu, \quad l' = \rho'\mu', \quad l_0 = \rho_0\mu_0, \quad \rho\sqrt{1-\mu^2} = \rho'\sqrt{1-\mu'^2} \quad (12)$$

and

$$l - l_0 = \eta, \quad l - l' = \eta - \eta'. \quad (13)$$

According to the last of these equations one can turn to integration over time in eq. (11) because $dl' = d\eta'$. As a result the formal solution (11) can be written as follows

$$\vec{n}(\rho, \mu, \eta) = \vec{n}_0(\rho_0, \mu_0)e^{-\int_0^\eta \alpha(\eta'')d\eta''} + \int_0^\eta \alpha(\eta')\hat{A}(\mu')\vec{s}_*(\rho', \eta')e^{-\int_{\eta'}^\eta \alpha(\eta'')d\eta''} d\eta', \quad (14)$$

taking into account eqs. (7), (12) and (13). Here vector $\vec{n}_0(\rho, \mu)$ defines initial (at the moment $\eta = 0$) distribution over distances and angles and

$$\rho_0 = \sqrt{\rho^2 - 2\rho\mu\eta + \eta^2}, \quad \rho_0\mu_0 = \rho\mu - \eta, \quad (15)$$

$$\rho' = \sqrt{\rho^2 - 2\rho\mu(\eta - \eta') + (\eta - \eta')^2}, \quad \rho'\mu' = \rho\mu - \eta + \eta'. \quad (16)$$

It follows from the formal solution (14) that one can introduce dimensionless time

$$u = \int_0^\eta \alpha(\eta')d\eta' = c\sigma_e \int_0^t n_e(t')dt' = c\sigma_e \int_z^{z_0} \frac{n_e(z')}{(1+z')H(z')} dz', \quad (17)$$

which has a sense of an optical distance (by Thomson scattering) between moments z and z_0 . Here redshift z_0 corresponds to the initial moment of time: $u = \eta = t = 0$ for $z = z_0$, n_e is an electron number density, $\sigma_e = 6.65 \cdot 10^{-25} \text{ cm}^2$ is the cross-section of Thomson scattering. For conformal time η we have equation

$$\eta = c \int_0^t dt'/a(t') = c \int_z^{z_0} dz'/H(z'), \quad (18)$$

which can be used to relate u with η by calculation both of them on the same grid of redshifts z . With the new time variable u the formal solution (14) takes the form

$$\vec{n}(\rho, \mu, u) = \vec{n}_0(\rho_0, \mu_0)e^{-u} + \int_0^u \hat{A}(\mu')\vec{s}_*(\rho', u')e^{u'-u} du'. \quad (19)$$

Substitution of eq. (19) into the righthand side of eq. (8) gives the following equation for $\vec{s}_*(\rho, u)$:

$$\vec{s}_*(\rho, u) = \vec{s}_0(\rho, u) + \frac{1}{2\rho} \int_0^u e^{u'-u} \frac{du'}{\eta - \eta'} \int_{|\rho-\eta+\eta'|}^{\rho+\eta-\eta'} \hat{A}^T(\mu) \hat{A}(\mu') \vec{s}_*(\rho', u') \rho' d\rho', \quad (20)$$

where arguments of matrices \hat{A}^T and \hat{A} are equal (according to eq. (16)) to

$$\mu = [\rho^2 - \rho'^2 + (\eta - \eta')^2]/[2\rho(\eta - \eta')], \quad \mu' = [\rho^2 - \rho'^2 - (\eta - \eta')^2]/[2\rho'(\eta - \eta')]. \quad (21)$$

Further the primary source vector in eq. (20) is

$$\vec{s}_0(\rho, u) = \frac{e^{-u}}{2\rho\eta} \int_{|\rho-\eta|}^{\rho+\eta} \hat{A}^T(\mu) \vec{n}_0(\rho_0, \mu_0) \rho_0 d\rho_0, \quad (22)$$

where

$$\mu = (\rho^2 - \rho_0^2 + \eta^2)/2\rho\eta, \quad \mu_0 = (\rho^2 - \rho_0^2 - \eta^2)/2\rho_0\eta. \quad (23)$$

according to eq. (15).

To deduce the main integral equation (20) we passed from integration over μ to integration over ρ' in the integral term and to ρ_0 in the free term using in the first case the first of eqs. (21) which gives

$$d\mu = -\rho' d\rho' / \rho(\eta - \eta'), \quad (24)$$

and in the second case we use the first of eqs. (23) which gives

$$d\mu = -\rho_0 d\rho_0 / \rho\eta. \quad (25)$$

In scalar case assuming isotropic scattering the main integral equation (20) has a more simple form

$$s(\rho, u) = s_0(\rho, u) + \frac{1}{2\rho} \int_0^u e^{u'-u} \frac{du'}{\eta(u) - \eta(u')} \int_{|\rho-\eta(u)+\eta(u')|}^{\rho+\eta(u)-\eta(u')} s(\rho', u') \rho' d\rho', \quad (26)$$

where

$$s_0(\rho, u) = \frac{e^{-u}}{2\rho\eta} \int_{|\rho-\eta|}^{\rho+\eta} n_0(\rho_0) \rho_0 d\rho_0, \quad (27)$$

and from eq. (19) we obtain for the formal solution:

$$n(\rho, \mu, u) = n_0(\rho_0) e^{-u} + \int_0^u s(\rho', u') e^{u'-u} du', \quad (28)$$

where

$$\rho_0 = \sqrt{\rho^2 - 2\rho\mu\eta + \eta^2}, \quad \rho' = \sqrt{\rho^2 - 2\rho\mu(\eta - \eta') + (\eta - \eta')^2}. \quad (29)$$

It should be stressed that in this case source function coincides with the mean (over angle variable) radiation intensity:

$$s(\rho, u) = j(\rho, u) \equiv (1/2) \int_{-1}^1 n(\rho, \mu, u) d\mu \quad (30)$$

Here and below the term "intensity" means dimensionless intensity i.e. photon occupation number.

As an initial condition we assume that at the moment $t = 0$ ($\eta = 0$) corresponding to some redshift z_0 radiation is nonpolarized and isotropic and has spherically-symmetrical distribution:

$$\vec{n}(\rho, \mu, 0) = (n_0(\rho), 0)^T, \quad (31)$$

where $n_0(\rho)$ is a given function which we take in the form

$$n_0(\rho) = \pi^{-3/2} \rho_*^{-3} \exp[-(\rho/\rho_*)^2] \rightarrow \delta(\rho)/(4\pi \rho^2) \quad \text{for } \rho_* \rightarrow 0, \quad (32)$$

where ρ_* is a parameter which can be taken sufficiently small to model point source. Obviously $n_0(\rho)$ satisfies to normalization

$$4\pi \int_0^\infty n_0(\rho) \rho^2 d\rho = 1. \quad (33)$$

We solve the problem of propagation of instantaneous burst of radiation in a scattering expanding and recombining Universe. Since albedo of Thomson scattering is equal to 1 the full number of photons emitted in the burst must be conserved. So that an equality

$$4\pi \int_0^\infty j(\rho, u) \rho^2 d\rho = 4\pi \int_0^\infty n_0(\rho) \rho^2 d\rho = 1. \quad (34)$$

must be fulfilled at any moment of time. One can make certain that this equality follows indeed both from vector equation (20) and scalar equation (26).

METHOD OF SOLUTION AND MAIN RESULTS

We obtained numerical solutions of vector equation (20) and scalar equation (26) by means of their discretization on given grids over dimensionless time u and over distance ρ measured in Mpc. It should be noted that the scale of distances ρ corresponds to the present epoch according to our normalization of scale factor: $a = 1$ at $z = 0$. As a main time grid we use a uniform grid over redshift z with the step $\Delta z = 10$ and grids over u and η are calculated then using eqs. (17) and (18). The function $\vec{s}_*(\rho', u')$ in the righthand side of integral equation (20) was approximated as a function of ρ' for fixed u' by cubic spline on a uniform grid with the step $\Delta\rho = 1$ Mpc and integral over ρ' was calculated analytically. Next the whole of integrand (except for exponential factor) in integral over u' was approximated (as a function of u') by quadratic spline and integral over u' was calculated analytically as well. At the last time point (for $u' = u$, $\eta' = \eta$) the whole integrand in integral over u' including the multiplier $1/2\rho$ turns to be equal to $\hat{B}\vec{s}_*(\rho, u)$ where $\hat{B} = \text{diag}(1, 7/10)$ is a diagonal matrix. Carrying this term of quadrature sum from the righthand side of equation to the lefthand one we get in the end recurrence relation which allows to express the current solution through solutions at the preceding moments of time. To control the process of solution we check up conservation of the full number of photons. It was fulfilled with a relative error no more than 10^{-7} for scalar equation and no more than 10^{-5} for vector equation.

After the source function was found then angular distributions of radiation intensity and polarization were calculated numerically from the formal solution for different distances from the center of the burst and at different moments (z) including the present one ($z = 0$). Calculations

were fulfilled for several values of initial moments of time in the range of redshifts z_0 from 1100 up to 3000.

The width of initial intensity distribution as a function of ρ (see eq. (32)) was taken to be $\rho_* = 1.5$ Mpc in the scale of distances at $z = 0$. But in the scale of distances corresponding to the moment of the burst (at some $z = z_0$) the width of initial distribution becomes (for $z_0 \gg 1$) much smaller: $r_* = a(z_0)\rho_* = \rho_*/(1 + z_0)$.

As regards to another parameters appearing in the problem they enter the Hubble factor in particular:

$$H(z) = H_0 \sqrt{\Omega_\Lambda + (1 - \Omega)(1 + z)^2 + \Omega_M(1 + z)^3 + \Omega_{rel}(1 + z)^4}, \quad (35)$$

where $H_0 = 2.4306 \cdot 10^{-18} h_0 \text{ s}^{-1}$, h_0 is the Hubble constant in the units of 75 km/(s·Mpc); Ω_M , Ω_Λ and Ω_{rel} are ratios of densities of matter, dark energy and relativistic particles (radiation, massless neutrino) to the critical density $\rho_c = 3H_0^2/(8\pi G)$ at the present epoch; $\Omega = \Omega_M + \Omega_\Lambda + \Omega_{rel}$, $\Omega_{rel} = \rho_R^0(1 + f_n)/\rho_c$, $\rho_R^0 = a_R T_0^4/c^2$ is a mass density of radiation at the present epoch (T_0 is the mean temperature of CMBR), f_n is a contribution of relativistic (massless) neutrino (usually $f_n = 0.68$). For the flat model of the Universe we have $\Omega = 1$ and then $\Omega_M = 1 - \Omega_\Lambda - \Omega_{rel}$.

Moreover number density of electrons enter the equations. It is measured usually in the units of the total number density n_H of hydrogen atoms and ions: $n_e(z) = x_e(z)n_H(z)$, where $x_e(z)$ is so called recombination history of the Universe and

$$n_H(z) = n_H^0(1 + z)^3, \quad n_H^0 = 0.63144 \cdot 10^{-5} X \Omega_B h_0^2^{-3}, \quad (36)$$

where Ω_B is a ratio of baryon density to critical density at the present epoch, X is a hydrogen abundance (by mass). Recombination history is calculated separately and enter as an input file. We calculated it using the programme "recfast.for" (Seager et al., 1999).

We adopted the following values of parameters: $\Omega = 1$, $\Omega_\Lambda = 0.7$, $\Omega_B = 0.04$, $T_0 = 2.728$ K, hydrogen abundance $X = 0.76$, $\Omega_{rel} = 0.85 \cdot 10^{-4}$, Hubble constant $H_0 = 70$ km/(s·Mpc).

Fig. 1 shows initial isotropic distribution of radiation. Results of calculations are shown in Figs. 2 – 7. Figs. 2 – 5 are obtained in scalar approximation and Figs. 6 and 7 – using exact description of scattering. Fig. 2 displays propagation of radiation wave generated by the burst at the epoch ($z = 10$ and 20) when the Universe was practically transparent for radiation (we do not consider here reionization connected with the birth of primary stars). Then radiation propagates freely and an interval between peaks in Fig. 2 is equal to the difference of conformal times of the burst for corresponding redshifts.

In Fig. 3 there are shown distributions of the mean intensity (i.e. source function) at the present epoch but for different moments (z_0) of the burst. Certainly all profiles are in the range of distances which do not exceed (strictly do not exceed if we neglect the width of initial spatial profile of the burst) conformal time of the burst (see Tabl. 1) since according to its definition (eq. (18)) conformal time is equal to a distance passed by freely flying photon from the moment of its emission (at some z_0) to the moment of its registration (at $z = 0$) in a fixed scale of distances coinciding by our choice with the scale in the present epoch. Also it is clear that distribution of diffuse radiation should be wider and its maximum should be nearer to the center of the burst as compared with straightly passed unscattered radiation which should have its maximum at a distance equal to conformal time of the burst. While maximum of diffuse radiation is situated according to our calculations at a distance $\rho = 13620$ Mpc irrespective of

the moment z_0 of burst beginning. This distance coincides as it is expected with the conformal time for the last scattering surface at $z \approx 1090$. This is illustrated by two-component profile in Fig. 3 for $z_0 = 1200$ containing both diffuse and straightly passed radiation.

Furthemore it is seen in Fig. 3 that for sufficiently large $z_0 \geq 2000$ the profile of distribution does not depend practically on the time of the burst beginning. Moreover our calculations show that it does not depend (providing that the full number of photons conserves) on a characteristic size of the burst (in our case this is parameter ρ_* in the initial distribution (32)) provided it is not too large (see below). So for sufficiently large z_0 the profiles of intensity distribution should be in a sense universal ones i.e. nondepending on initial conditions of the burst as it was indicated earlier by Dubrovich (2003). This is connected with the large optical thickness of the Universe by Thomson scattering at large redshifts (see Tabl. 1). So that photons emitted during the burst are trapped and a size of radiating region changes due to diffusion not too much till the moment of sufficient clearing of the Universe at $z \approx 1200$ owing to hydrogen recombination.

It should be noted that in accordance with our solution normalization on the full number of photons emitted during the burst into space the calculated quantities have a dimension of inverse volume, namely 1 Mpc^{-3} . Therefore if at the moment of the burst its central intensity (at $\rho = 0$) is equal to n_0 then our profiles must be multiplied by $\pi^{3/2}n_0(\rho_*/1\text{Mpc})^3$ according to the form of our initial profile (eq. (32)). But in general case taking into account weak dependence of solution on the initial conditions one can take as a transitional multiplier e.g. $(4\pi/3)\bar{n}(\rho_0/1\text{Mpc})^3$ where ρ_0 is a typical size of the burst and \bar{n} is intensity averaged in a sphere of this size.

In Fig. 3 one can see also that as redshift z_0 approaches to the beginning of hydrogen recombination the changes of the profile become more and more appreciable and during recombination when clearing of the medium becomes noticable the straightly passed unscattered radiation of the burst appears: at $z_0 = 1200$ it is seen as a narrow peak to the right of diffuse maximum and at $z_0 = 1100$ it is already dominates (see Fig. 4).

In Fig. 5 one can see angular distributions of radiation intensity at different distances from the center of the burst and at different moments (z_0) of the burst (see Tabl. 2). Characteristic feature of these distributions is their small width (3 – 10 arcminutes) and the width is smaller on the leading front than on the rear one and it decreases with the growth of z_0 . It should be stressed that owing to such a strong anisotropy the radiation intensity towards the center of the burst can be almost 10^7 times larger than angle averaged intensity (see Tabl. 2 and Fig. 3). It is clear that degree of diffuse radiation anisotropy is defined by an angle $2\vartheta_d$ at which radiating region is seen at the present epoch ($z = 0$) on the last scattering surface ($z_{\text{ls}} \approx 1090$, $\eta_{\text{ls}} \approx 13620 \text{ Mpc}$). If r_d is the region radius at that moment then obviously $\mu_d = \cos \vartheta_d \sim r_d/\eta_{\text{ls}}$ for $r_d = \rho_d/(1 + z_{\text{ls}}) \ll \eta_{\text{ls}}$. For straightly passed radiation the cosine of angle at which the burst (arised at $z = z_0$) is seen at a distance ρ from the center amounts $\mu_r = \cos \vartheta_r \sim r_*/\rho$ for $r_* = \rho_*/(1 + z_0) \ll \rho$ where ρ_* is the initial radius of the burst in the present scale of distances. For example for the burst at $z_0 = 1100$ we have $\rho = \eta \approx 1.36 \cdot 10^4 \text{ Mpc}$ taking $\rho_* = 1.5 \text{ Mpc}$ for the initial radius of the burst. So that we have $\mu_r \approx 10^{-7}$ and $\vartheta_r \approx 1.5$ arcminutes. In this case as was already pointed above the main part of radiations comes to us without scattering on the way. As for diffuse radiation which dominates for $z_0 > 1200$ the width of its angular distribution turns out to be larger. Thus for $z_0 \geq 1600$ the semiwidth of angular distribution of radiating region at $z = 0$ is equal to 3 – 10 arcminutes according to our calculations so that its

z_0	u	η , Mpc
3000	177.23	13770
2000	67.63	13720
1600	29.27	13686
1400	12.74	13664
1200	3.01	13635
1100	1.07	13618

Table 1: Optical distances u and conformal times η of the burst from its beginning at z_0 to the present epoch $z = 0$.

N	r , Mpc	$z_0 = 1600$	$z_0 = 2000$	$z_0 = 3000$	$z_0 = 2000$
1	13570	$1.02 \cdot 10^{-6}$	$1.02 \cdot 10^{-6}$	$1.02 \cdot 10^{-6}$	$1.27 \cdot 10^{-6}$
2	13600	$6.91 \cdot 10^{-6}$	$6.56 \cdot 10^{-6}$	$6.28 \cdot 10^{-6}$	$7.39 \cdot 10^{-6}$
3	13630	$1.92 \cdot 10^{-5}$	$1.57 \cdot 10^{-5}$	$1.38 \cdot 10^{-5}$	$1.69 \cdot 10^{-5}$
4	13660	$6.97 \cdot 10^{-7}$	$7.89 \cdot 10^{-7}$	$8.60 \cdot 10^{-7}$	$9.00 \cdot 10^{-7}$

Table 2: Radiation intensity $n(0)$ towards the center of the burst as a function of distance r from the burst center for different moments z_0 of the burst beginning. Last column corresponds to exact description of Thomson (Rayleigh) scattering and preceding three columns correspond to scalar approximation.

radius at $z = 1100$ must be 2 – 7 times larger than for the burst at $z_0 = 1100$ i.e. $\rho_d \approx 3 - 10$ Mpc in the present scale of distances and $r_d = \rho_d/(1 + z_0)$ in the scale of distances at $z = z_0$. Therefore the characteristic initial radius of the burst at $z_0 \geq 1600$ must be in any case smaller than this estimate lest it should influence vitally on the properties of the burst radiation at the present epoch.

Further, decrease of anisotropy when passing from the "base" of leading wave front over maximum to the "base" of rear front (see Fig. 3 and Tabl. 2) is explained as follows: photons observed at the largest distances come from the nearest part of radiating region in a small solid angle and an effective size of region giving a contribution to observed radiation grows with the distance decrease.

Fig. 6 shows change of angular distributions when passing from approximate scalar description of Thomson scattering to an exact description taking into account scattering anisotropy and polarization. Finally Fig. 7 shows that polarization of radiation can be rather large (up to 70%) but on angular distances where radiation intensity becomes already much smaller than towards the center of the burst (see preceding Figure). It should be noted also anticorrelation between polarization and anisotropy of radiation. Namely, when passing from the farthest (from the burst center) point of the wave profile to the nearest one an anisotropy decreases but polarization grows (cf. Figs. 6 and 7). The thing is that radiation from farthest points comes from the nearest to observer small part of emitting region and mainly it consists of photons undergone their last scattering almost directly forward which changes polarization only slightly. But for the less distant (from the burst center) points an essential contribution comes from photons scattered under sufficiently large angles which leads to polarization growth.

CONCLUSIONS

A source of very small size radiating energy in prerecombination epoch will be seen now as a some spot on the background of cosmic microwave radiation. Our calculations confirm initial conclusion made by Dubrovich (2003) about nondependence of angular size of this spot on the moment of the source burst on condition that it is situated at a distance of optimal visibility. For estimates of radiation intensity it is important that duration of the source burst also has a very little influence on the size of the spot. More exactly, it takes place for the time interval before the moment of the Universe clearing due to hydrogen recombination. Assuming that the burst radiation has no effect on the medium parameters the burst size does not depend also from the burst power. Calculated exact profiles of intensity distribution give an opportunity to determine relation between angular size of a spot and physical distance to a source. Very important feature is also a presence of radiation polarization in the spot. Polarization is standard one for the case of star radiation scattered in a shell of gas with free electrons. The plane of polarization contains the ray of sight and direction towards the star center. Degree of polarization grows when moving off a spot center. However the most probable observed polarization degree will be about 15% on average because of fast brightness decrease to the edge of a spot.

This research is supported by Russian Foundation for Basic Research (grant 08-02-000493).

REFERENCES

1. Dubrovich V.K., *Astronomy Letters* **29**, 6 (2003).
2. Ivanov V.V., *Astron. Astrophys.* **303**, 609 (1995).
3. Nagirner D.I., Kirusheva S.L., *Astronomy Reports* **49**, 167 (2005).
4. Nagirner D.I., Kirusheva S.L., *Astronomy Reports* **54**, 55 (2010).
5. Seager S., Sasselov D.D., *Astrophys. J.* **523**, L1 (1999).

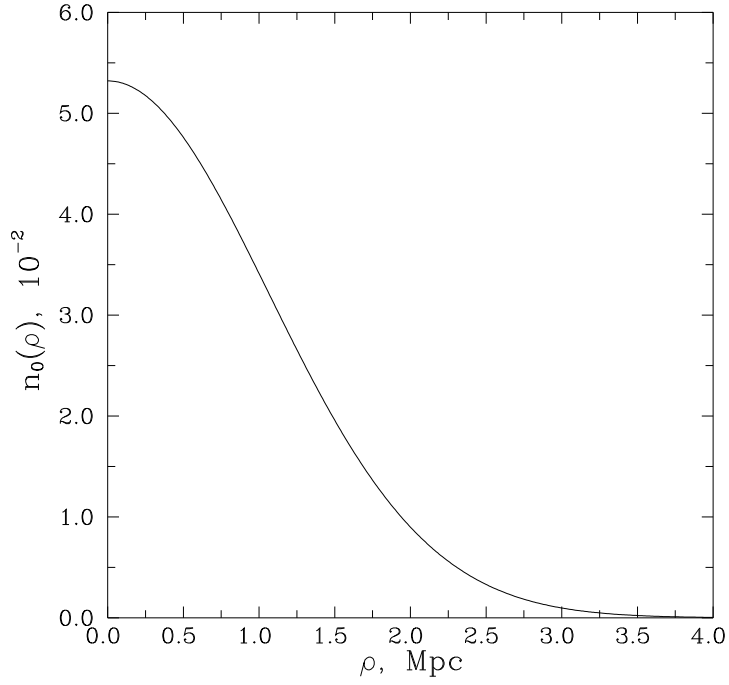


Figure 1: Initial (isotropic) distribution of radiation intensity.

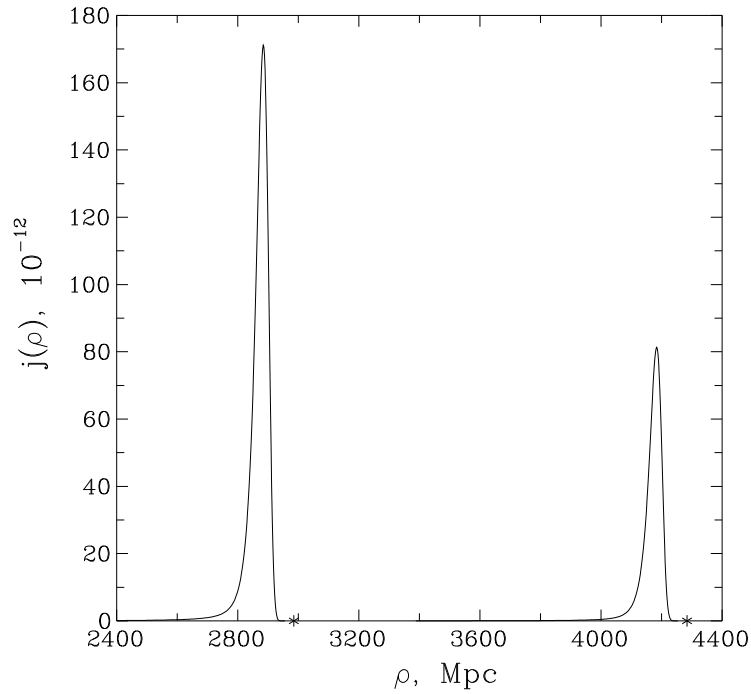


Figure 2: Distributions of the mean intensity at $z = 10$ (left profile) and $z = 20$ (right profile) ($z_0 = 2000$). Asterisks on the abscissa mark distances equal to conformal times of the burst for corresponding z .

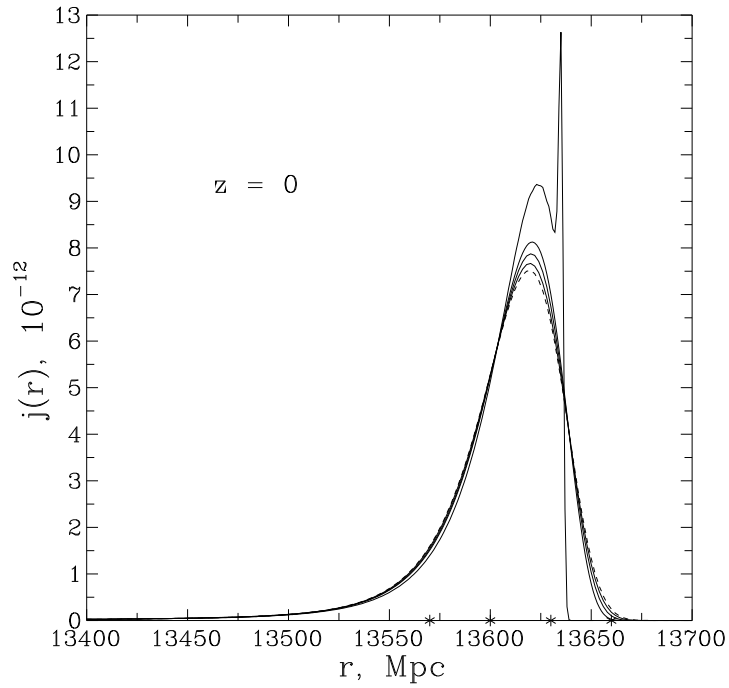


Figure 3: Distributions of the mean intensity at the present epoch for different z_0 . In the order of maximum intensity growth they correspond to $z_0 = 3000, 2000, 1600, 1400$ and 1200 . In the same order the steepness of the leading (right) front of distribution grows. Asterisks on the abscissa mark distances indicated in Tabl. 2.

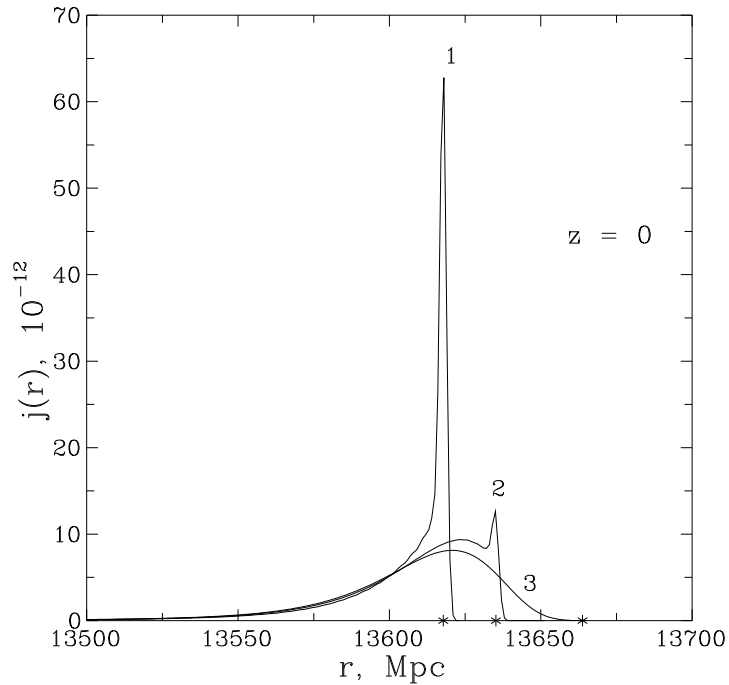


Figure 4: The same as in the preceding Figure but for $z_0 = 1100$ (1), 1200 (2) and 1400 (3). Asterisks mark corresponding conformal times of the burst (see Tabl. 1).

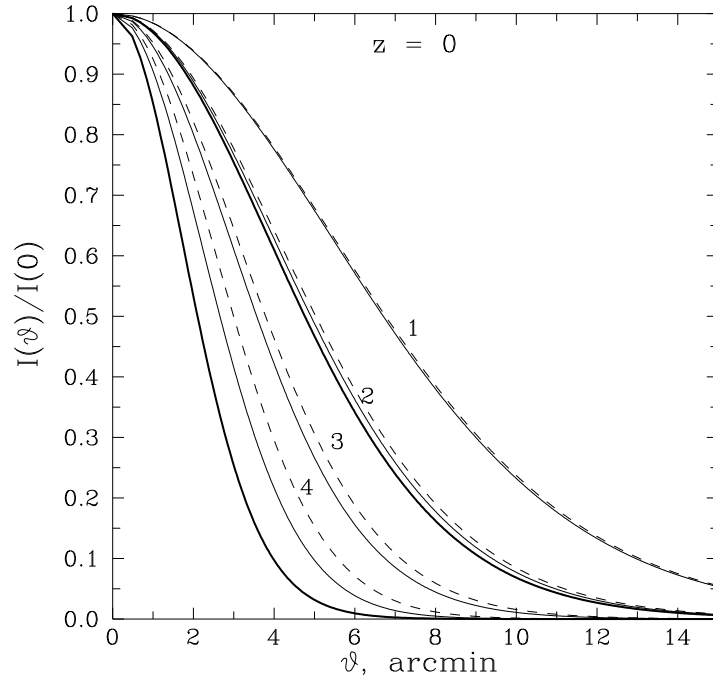


Figure 5: Angular distributions of radiation intensity at $z = 0$ at different distances r (see Tabl. 1) from the burst center and for different z_0 : thin continuous lines – $z_0 = 2000$, dashed lines – $z_0 = 3000$ and thick continuous lines – $z_0 = 1600$ (for two distances – $N = 4$ and 2 in Tabl. 2). Here ϑ is an angular distance from the burst center.

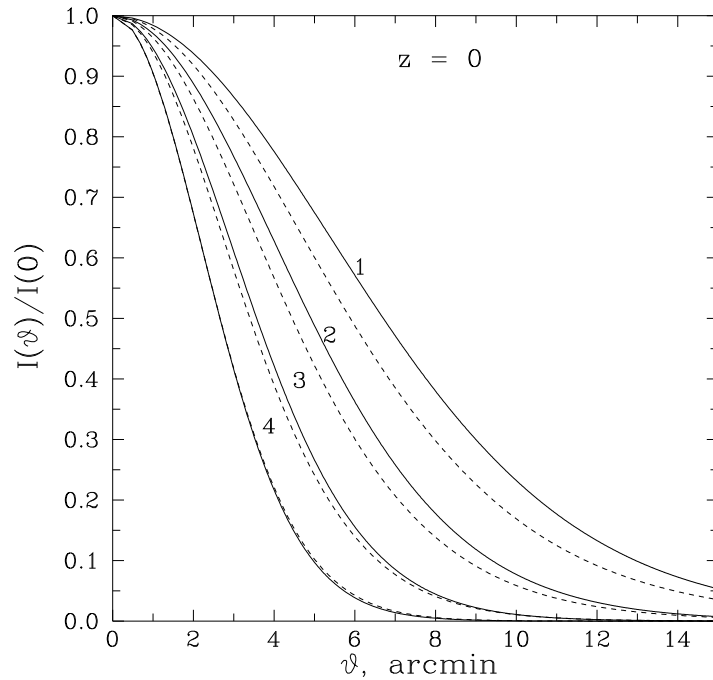


Figure 6: The same as in the preceding Figure for $z_0 = 2000$ in scalar approximation (continuous lines) in comparison with distributions for exact description of Rayleigh scattering (dashed lines).

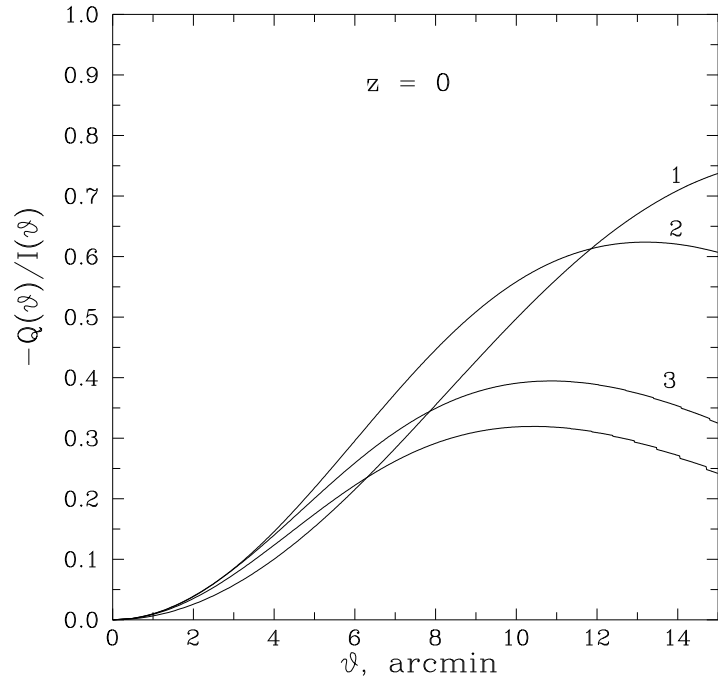


Figure 7: Angular distributions of radiation polarization at $z = 0$ at different distances r from the burst center (designations are the same as in the preceding Figure). Lowest (with the smallest maximum) curve corresponds to distance 13640 Mpc.